Journal of Molecular Liquids 368 (2022) 120823

Contents lists available at ScienceDirect

Journal of Molecular Liquids

journal homepage: www.elsevier.com/locate/molliq

Low-temperature processable transparent liquid crystal light shutter

Young Jin Lim [a], Minji Kang [a], Hyun Soo Jeon [a], MinSu Kim [a,*], Seung Hee Lee [a,b,*]

[a] Department of Nano Convergence Engineering, Jeonbuk National University, Jeonju, Jeonbuk 54896, Republic of Korea
[b] Department of Polymer Nano Science and Technology, Jeonbuk National University, Jeonju, Jeonbuk 54896, Republic of Korea

ARTICLE INFO

Article history:
Received 8 September 2022
Revised 16 October 2022
Accepted 15 November 2022
Available online 19 November 2022

Keywords:
Low-temperature process
Polyimide-free alignment
Liquid crystals
Reactive mesogens
Normally transparent smart windows

ABSTRACT

Tunable light shutters show their great potential as smart windows, especially when energy efficiency is greatly entailed. Polymer-dispersed liquid crystals (PDLCs) are one of the most well-known and promising methods for smart window applications, but there are many obstacles to overcome or to develop further. At first, PDLCs require high voltages not only when to switch from an opaque to a transparent state but also to maintain the transparent state. A transparent mode, which can be produced by polymer-stabilizing homeotropic alignment of LCs, can be one of the ways to reduce energy consumption significantly from this perspective. However, the most efficient material for the induction of the homeotropic alignment, polyimide requires high temperature for the surface treatment process. Here we demonstrate a low-temperature process for plastic substrates, allowed via a homeotropic alignment induction molecule, premixed in LCs. The mixture before polymerization contains LCs, a reactive mesogen, and a homeotropic alignment inducer. The homeotropic alignment inducer plays a role of polymer-stabilization as well. We believe the result clearly suggests a novel approach to resolve the issues in establishing initial structures and energy consumption of PDLCs for smart windows.

1. Introduction

In response to the global energy-saving policies, energy-efficient smart windows are rapidly and widely spreading in buildings and automobiles. Liquid crystal (LC) based smart windows can be switched between opaque (scattering) and transparent (transmitted) states, and they are one of the most widely used methods in this purpose. Polymer-dispersed liquid crystal (PDLC) or polymer-networked liquid crystal (PNLC) are representative examples and classified in general depending on morphology of their polymer network. The polymer morphology is highly related to the concentration of monomers to LCs and is highly dependent on how phase separation occurs during the polymerization. In general, the concentration of 20–50 wt% in PDLC devices results in the formation of LC droplets whose size is 0.4–30 μm [1,2]. Considering energy efficiency, PDLC devices consume high power because biased voltage is required to keep the transparent mode, like normal glass windows [1–6]. When the concentration of monomers is less than 10 wt%, polymer network is formed without LC droplets and their morphology follows the initial alignment of LCs, which is determined by the surface treatment. In this way, we can realize a transparent PNLC mode as it is studied intensively in recent days [7–9] and can find more reports utilizing homeotropic alignment and negative dielectric isotropic LCs to reorient LCs in the plane of substrates [6,8,10–13]. However, in these normally transparent PNLCs, a polyimide alignment layer is required. The coating of the polyimide requires high-temperature baking process about 200 °C, which may restrict the use of plastic substrates.

Removing the polyimide layer results in cost-efficient, short-processing time, and the low-temperature processing extends the application to plastic substrates. To induce homeotropic alignment of LCs without the polyimide layer, LCs are mixed with additional materials to function at the interface between LC and substrates. Recent works have reported approaches to induce the homeotropic alignment using nanoparticles, such as polyhedral oligomeric silsesquioxane (POSS) [14–16], octadecyltrichlorosilane (OTS) [12], hexadecyltrimethyammonium bromide (HTAB) [11]. These reports using nanoparticles show a good homeotropic alignment [12].

In this work, we demonstrate a LC light shutter, for a smart window, with normally transparent PNLC mode, replacing polyimide by a homeotropic alignment material (HAM), which possesses two roles of a homeotropic alignment inducer and photopolymerizable reactive mesogen (RM) [17,18]. The HAM molecules are easy to disperse in LCs, and the fabrication step can be reduced because additional steps for the surface treatment are not required.

* Corresponding author.
E-mail addresses: minsu.kim@jbnu.ac.kr (M. Kim), lsh1@jbnu.ac.kr (S.H. Lee).

https://doi.org/10.1016/j.molliq.2022.120823
0167-7322/

Amorphous or random morphology of polymer networks in LC-polymer composite systems often bring about hysteresis on electro-optic characteristics upon LC reorientation. For example, blue phase liquid crystal (BPLC) [19–22], optically isotropic liquid crystal (OILC) [20,23–26], and PDLC [27] require high fraction of polymers to LCs in order to sufficiently hold the LC alignment. On the other hand, it seems relatively low concentration of polymer is sufficient because the initial LC orientation for polymer-stabilization in PNLC does not cost much elastic energy even if LCs are homeotropically and uniformly aligned via HAM. When single-sided UV irradiation still reaches the bounding substrate with appropriate cell gap (about less than 5 μm), small amount of polymers need to be formed on a substrate to hold initial LC orientation [18]. However, our proposed PNLC mode requires a little higher amount of polymer because the polymer network should be formed across the cell thickness direction. Thus, it is important to verify the hysteresis in PNLC system owing to the high-polymer concentration [28] and to clarify the possible effect of unit cell aging. We can resolve this issue by optimizing the polymerization condition: the energy and geometry of UV irradiation. We show hysteresis-free upon electric field strength-dependent haze measurement with good transparent and opaque states. We confirmed that the overall process was possible in room temperature.

2. Materials and methods

We prepared PNLC composites that consist of LC with negative dielectric anisotropy ($\Delta\varepsilon$ = -1.99, n_e = 1.748, n_o = 1.513, JNC Korea Co., Ltd.), HAM 1 wt% to the host LC, RM (RM257, n_e = 1.687, n_o = 1.508, Merck), and a photo-initiator (Irgacure651, Sigma-Aldrich) 0.5 wt% to the RM. The chemical structure of HAM, Irgacure651, and RM are shown in Fig. 1(a). The mixture LC:RM was capillary-injected in between two indium-tin oxide (ITO) coated glass substrates as shown in Fig. 1(b). Right after the mixture was injected into the cell, we believe the HAM molecules spontaneously migrate onto the surface, and they induce homeotropic alignment of the LC and thus the RM molecules. After confirming the homeotropic alignment, UV light was irradiated onto single side or two sides of cells with the cell gap $d \sim 10$ μm (Fig. 1(c)) at 50 mW cm^{-2} for an hour unless otherwise mentioned. Upon the UV exposure, the RM and HAM were polymerized, and polymer network was formed uniformly over cells. To measure transmittance and haze as a function of applied voltage, a commercial electro-optic measurement system (LCMS 200, Sesim Photonics Technology) and a haze meter (COH 400, Nippon Denshoku) was used and UV–vis spectrum was measured by using a UV–vis spectra photometer (S-3100, Scinco). The polymer networks were observed by FE-SEM (SUPRA40VP, Carl Zeiss) installed in the Center for University-wide Research Facilities (CURF) at Jeonbuk National University.

3. Switching principle

The switching principle of the proposed normally transparent PNLC cell is shown in Fig. 2 when voltage is off (Fig. 2(a)) and on (Fig. 2(b)). The transparent mode is achieved via polymer-stabilized homeotropic alignment of LCs. We estimate difference of the ordinary refractive index between the LCs and RMs as $n_{o,RM} - n_{o,LC} \sim 0.005$ and ensure that the scattering occurs at the interface is minor although the uniformity of the RM alignment would slightly drop after polymerization. With voltage applied between top and bottom ITO layers, LC with negative dielectric anisotropy

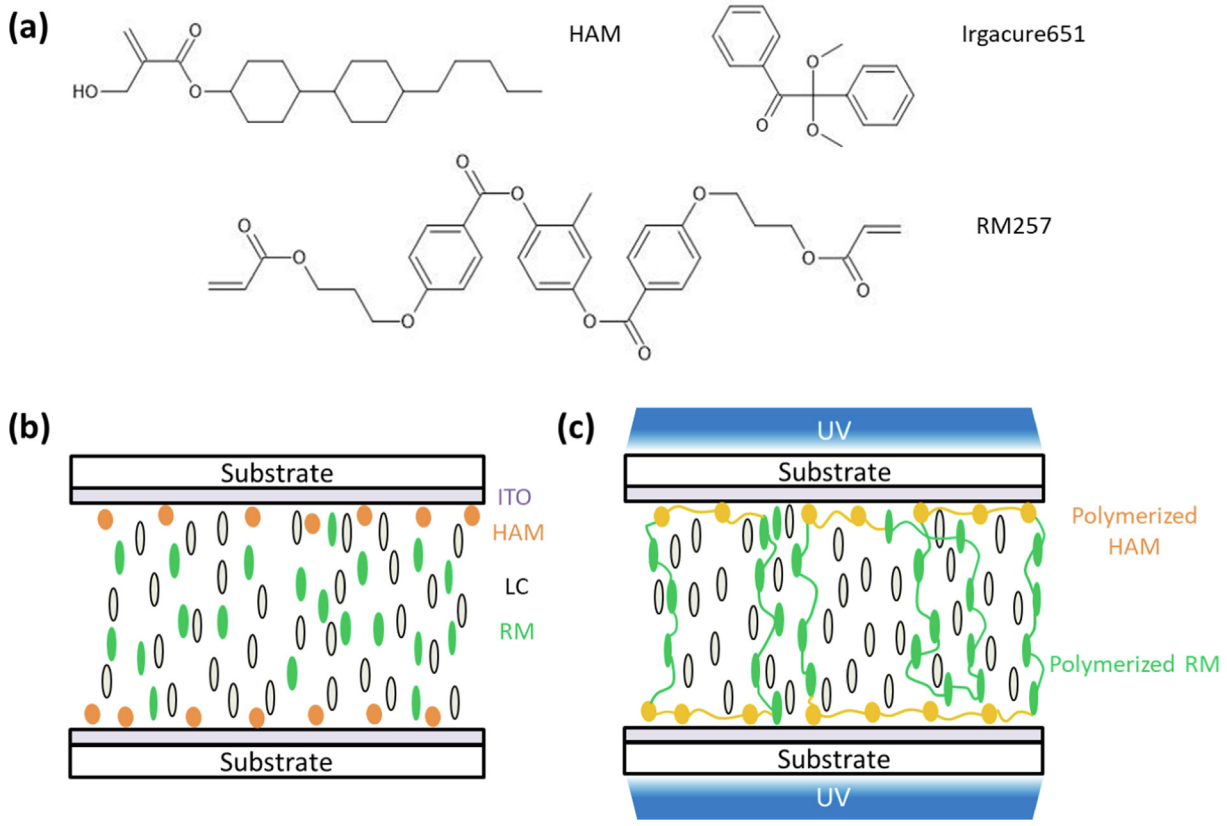

Fig. 1. (a) Chemical structures of the materials used for the homeotropic alignment of LC and polymer network. Schematics of the fabrication process to achieve normally transparent PNLC via homeotropic alignment of LCs: (b) the initial state after injection of LC mixtures; (c) polymerization by UV exposure on both sides of the cell.

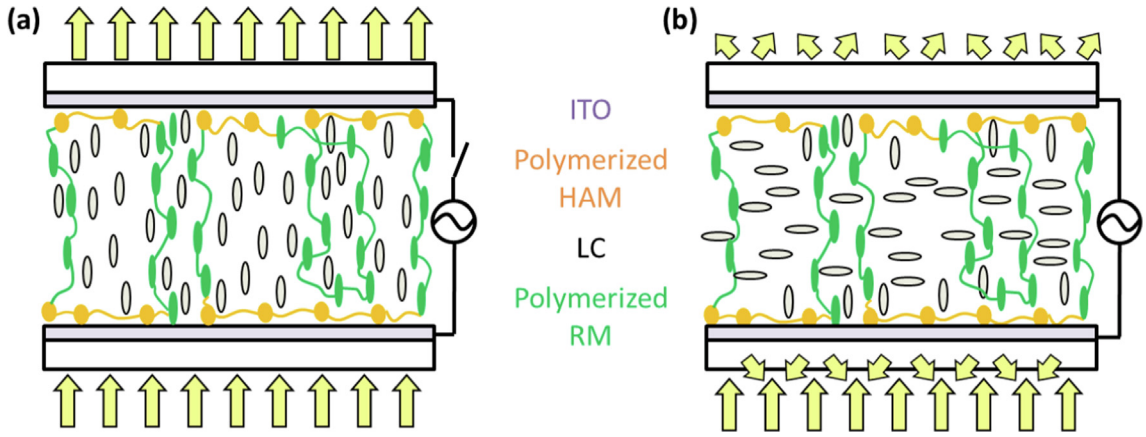

Fig. 2. Switching mechanism of normally transparent PNLC (a) transparent and (b) opaque state.

reorients into the plane of the substrates with random azimuthal orientation owing to the polymer network as shown in Fig. 2(b). In this state, the refractive index difference becomes $n_{e,LC} - n_{o,RM} \sim 0.24$ so that scattering occurs.

4. Results and discussion

Fig. 3(a) shows electric field strength-dependent haze curves with respect to the RM concentration. When the RM concentration varies by 3, 6, and 10 wt%, the electric field strength-dependent haze curves show 3.0, 3.8, 4.7 % of haze at the turn-off state. As the electric field strength increases, optical scattering begins to occur and the scattering gets significant at the interfaces between LC and polymer network, and the haze is measured by 75.1, 84.3, and 83.4 %, respectively, at 8 V μm^{-1}. From the result, RM 6 wt% was selected for further study for further improvement because we found that the transparency and opacity are optimized in this concentration.

Fig. 3(b) shows electric field strength-dependent haze curves of the cell when the host mixture is mixed with 6 wt% of RM. We observed hysteresis of the cell in the first three measurements but verified that the aging of cells can help reducing the hysteresis. At first, we explored the electro-optic performance of a cell with single-sided UV irradiation at 5 mW cm^{-2} for 10 min. We increased the electric field strength from 0 to 10 V μm^{-1}, and measured the haze, but the turn-off haze significantly increases as per repeating the measurements. After aging the cell by repeating the electric field strength sweep, the turn-off haze is partially but not fully recovered. The LC directors might be unable to return to the original homeotropic alignment. From this result, we can verify that the original LC alignment is unrecoverable even after 30 min of relaxation. To improve this, we moved onto exploring the effect of polymerization condition.

To form polymer network that can fully turn the original LC orientation back, we focused on exploring the effect of UV exposure energy as shown in Fig. 4. We measured electric field strength-dependent haze curves of cells with various polymerization condition by varying UV intensity and exposure time, 5 mW cm^{-2} for 20 min (Fig. 4(a)), 50 mW cm^{-2} for 20 min (Fig. 4(b)), and 50 mW cm^{-2} for an hour (Fig. 4(c)). Although the results show enhancement, the hysteresis still exists. We thus consider the geometry of UV exposure, in a way that the UV is irradiated on both sides of the sample cell to eliminate any possible asymmetric formation of polymer networks along the cell thickness direction or any incomplete remaining monomers or oligomers. As a result, shown in Fig. 4(d), the hysteresis is reduced significantly, whose degree is quantified as in Table 1.

In Fig. 4(e), we measured the optical spectrum of the cell from Fig. 4(d) in the visible wavelength. As increasing the electric field strength, overall transmittance decreases with no specific peak owing to optical scattering, which means the opaque state effectively interferes the visibility over the entire visible wavelength range.

As the transparent and scattering modes are mainly dependent on how the refractive indices of LC and RM, the haze property of the transparent state can be interfered in an oblique view. Thus,

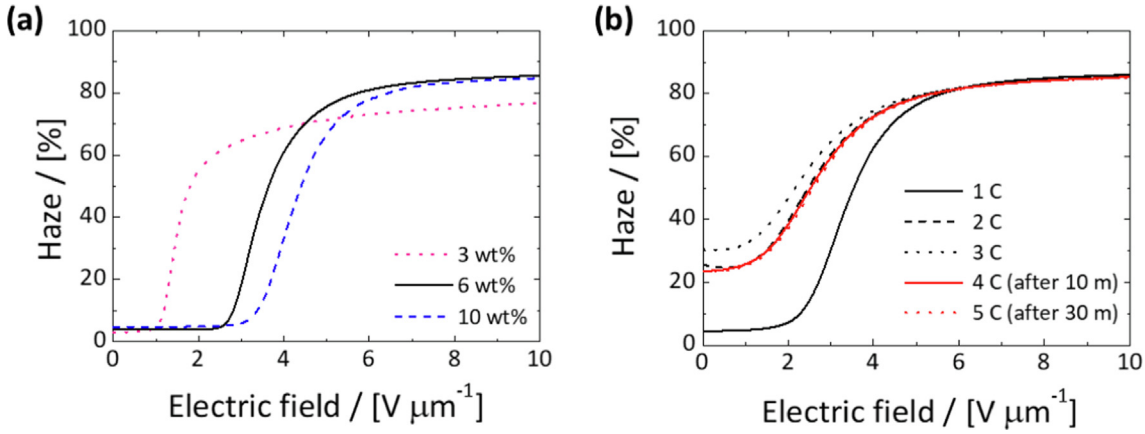

Fig. 3. Electric field strength-dependent haze curves of the normally transparent PNLC. (a) When the RM concentration varies. (b) After aging process of the RM 6 wt% cell.

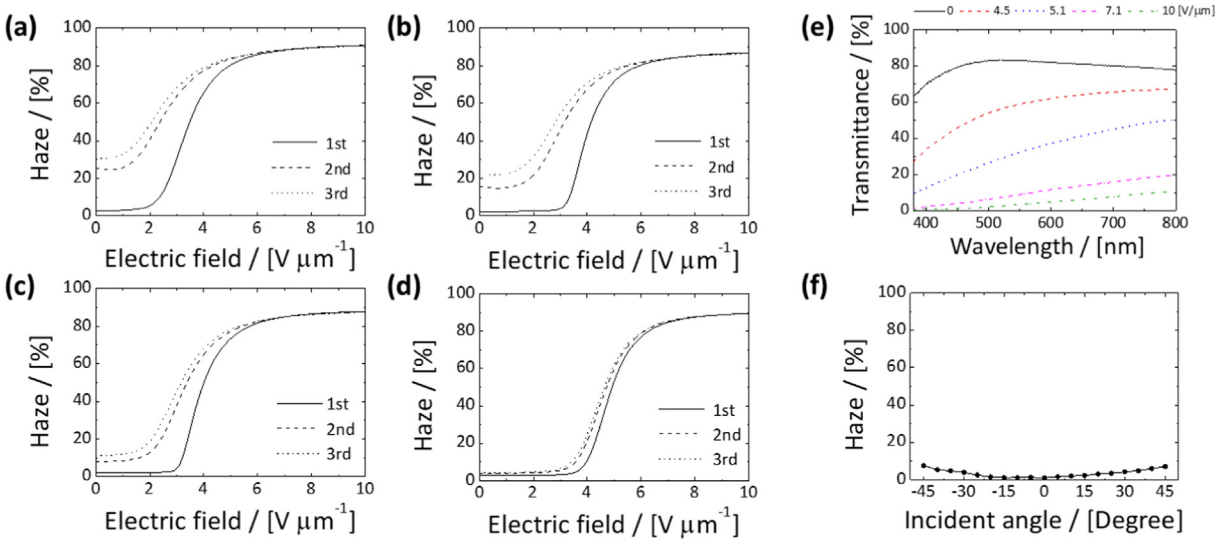

Fig. 4. Hysteresis minimization verified by the electric field strength-dependent haze measurement for various UV exposure conditions when sweeping the cells in the first, second, and third cycles. (a–c) UV exposure onto a single side of the cells at (a) 5 mW cm^{-2} for 20 min, (b) 50 mW cm^{-2} for 20 min, and (c) 50 mW cm^{-2} for an hour. (d) UV exposure onto both sides of the cell at 50 mW cm^{-2} for an hour. (e) Visible wavelength spectrum of the cell from (d) with respect to the electric field strength. (f) Haze measured in oblique incident angles.

Table 1
The quantified hysteresis.

UV irradiance [mW cm^{-2}]	5	50	50	50
Exposure time [min]	20	20	60	60
UV irradiation side	single	single	single	double
[a]$H_{1\text{-}2}$ [%]	7.2	8.4	6.1	1.8
[b]$H_{2\text{-}3}$ [%]	1.2	1.8	1.9	0.6

[a] $H_{1\text{-}2}$: Hysteresis between the first and second measurements.
[b] $H_{2\text{-}3}$: Hysteresis between the second and third measurements.

we measured the haze in various incident angles as shown in Fig. 4 (f). The measured haze at the normal view, at the incident angle, 0°, is ~0.95 %, and it increases up to ~7 % at the incident angle, ±45°. This increase in the haze level at oblique angles occurs from the difference between $n_{o,LC}$ and $n_{o,RM}^{eff}$ as explained in the switching principle.

Fig. 5 shows polarized optical microscopic (POM) and conoscopic images of the cells to investigate the original alignment of LC within polymer network and the hysteresis by observing the transparent state of the cells before UV exposure and after sweeping electric field strength to the polymer-networked cells of single-sided and double-sided UV exposures. Before UV exposure, we can observe that LC molecules are homeotropically aligned by HAM as shown in Fig. 5(a,b). When the sample cells are placed in between crossed polarizers, the transparent mode shows a dark state, and the Maltese cross of isogyres in the conoscopic mode is shown to suggest the uniformity in the homeotropic LC alignment. After polymerization and the first sweeping of the electric field strength, we observed weather the initial dark state is sufficiently recovered: in the case of single-sided UV exposure, the dark state is not achieved as shown in Fig. 5(c). In the case of double-sided UV exposure, however, the dark state is almost recovered as shown in Fig. 5 (d).

We took photographs of the sample cells to verify the scattering mode achieved by applying voltage when the cells are fabricated under the UV exposures on single side and double sides of the cells at 50 mW cm^{-2} for an hour and placed 2 cm away from a printed image as shown in Fig. 6. When the turn-off state of each cell shows the transparent state, the printed images are viewed clearly. Upon ramping up the electric field strength, the samples turn into scattering modes and the printed image becomes hazy owing to refractive index mismatching between LC and the polymer network. The sample cell with single-sided UV exposure becomes hazy at 4 V μm^{-1} (Fig. 6(a)) whereas the sample cell with double-sided UV exposure becomes hazy at 6 V μm^{-1} (Fig. 6(b)). The larger surface area on both sides covered by polymer networks in Fig. 6(b) can strengthen the anchoring of LC to the surface harder than that in Fig. 6(a), and thus, the original LC alignment is relatively well recovered in Fig. 6(b).

To verify how the polymer network is formed for two-different UV exposure conditions, we observed the field emission scanning electron microscope (FE-SEM) as shown in Fig. 7. After removing LC from the polymer network by soaking the cells in solvents (*n*-Hexane), we cut the cells in a way that we maintain substrates attached and keep the polymer network not collapsed. As we expected the single-sided UV exposure gives the polymer network on only top substrate, but the double-sided UV exposure clearly produces the polymer network on both top and bottom substrates. The cross-sectional view clarifies it as we observe the polymer network connected from top to bottom substrate as shown in Fig. 7(b).

We finally confirmed that the demonstrated cells show greater electro-optic properties than those using polyimide alignment layers. As shown in Fig. 8, the cell fabricated by using HAM shows the threshold electric field strength at 3.8 V μm^{-1} and the haze is achieved up to ~90 % at ~9 V μm^{-1}. The cell using polyimide shows the threshold electric field strength at ~4.8 V μm^{-1} and reaches the haze ~85 % at ~10 V μm^{-1} as shown in Fig. 8(a). The cue parameters for adjusting or optimizing the haze or clear level would be the cell thickness and matching refractive indices of LC and RM. For example, to enhance the haze level, the cell thickness

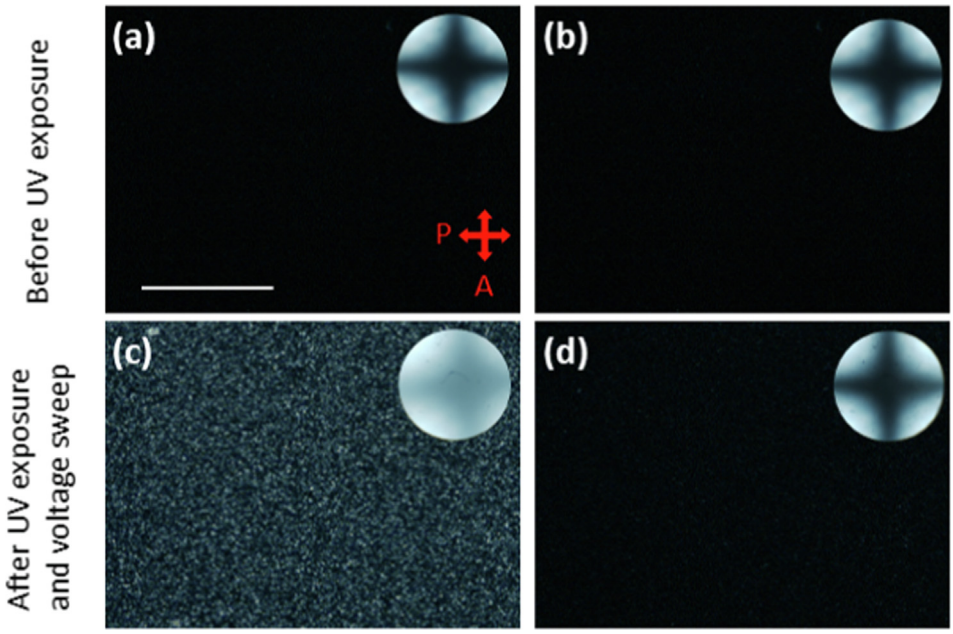

Fig. 5. Polarized optical microscopic (POM) and conoscopic images of the cells (a, b) before UV exposure and (c, d) after UV exposure and one time voltage sweep when the UV exposed on (a,c) a single and (b,d) double sides of the cells at 50 mW cm^{-2} for an hour. The scale bar is 200 μm.

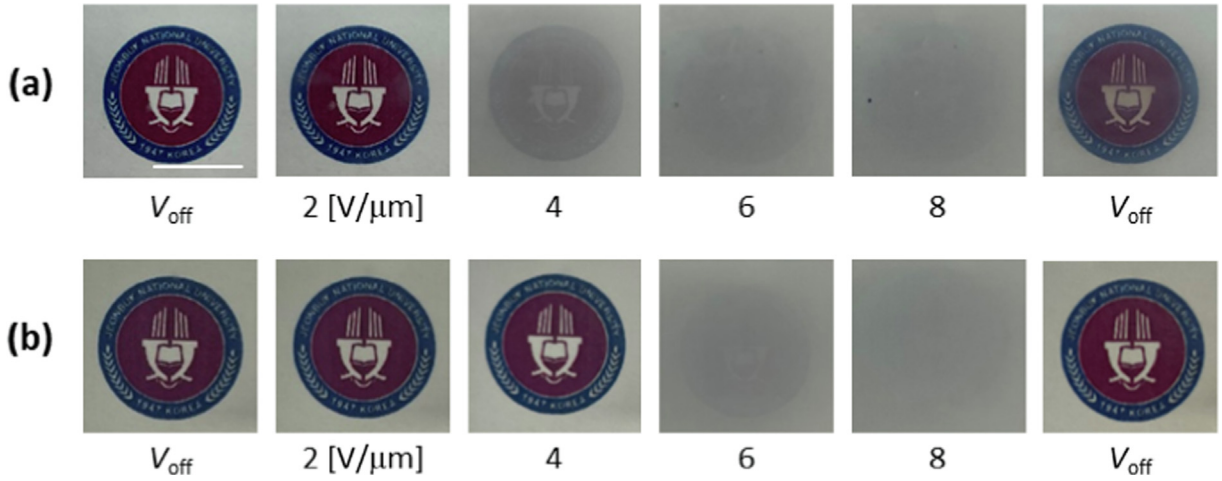

Fig. 6. Photographs of sample cells, fabricated by (a) single-sided and (b) double-sided UV exposures at 50 mW cm^{-2} for an hour. The scale bar is 2.5 cm, and the cells are 2 cm away from a printed image.

would be increased while matching the ordinary and extraordinary refractive indices of LC and RM. In addition, we measured time-dependent transmittance of both cells as shown in Fig. 8(b). The cell with HAM shows the turn-on time $\tau_{on} \sim 5$ ms and turn-off time $\tau_{off} \sim 2.5$ ms, and the cell with polyimide shows $\tau_{on} \sim 5.1$ ms and $\tau_{off} \sim 2.6$ ms. We have greater electro-optic property in the electric field strength-dependent haze measurement with the cell using HAM than polyimide and similar result in the time-dependent transmittance measurement.

5. Conclusion

We demonstrate polymer-networked liquid crystal (PNLC) cells that show an initially transparent state for energy efficiency and polyimide-free low-temperature processable method. The LC mixture consists of LC (negative dielectric anisotropy), reactive mesogen (RM), and homeotropic alignment material (HAM) which can induce the homeotropic alignment of LCs without any surface treatment. The results clearly show that UV irradiation on both sides of the cells enables us to produce robust polymer network for the best electro-optic properties. We can verify not only the initial homeotropic alignment, a transparent state is well achieved but also the hysteresis becomes almost eliminated. We believe it can provide possible way to realize a smart window that does not require power consumption to keep the transparent state, which overcomes one of the shortcomings of polymer-dispersed liquid crystal (PDLC) while achieving a good opaque state up on applying voltage. In addition, the use of HAM molecules enables polyimide-free fabrication process, that is, no high-temperature treatment is required to induce homeotropic alignment of LCs. It can highly enhance the fabrication efficiency, including cost, time, and most importantly, opening the applicability to plastic substrates. We believe this proposed device can open a novel way to

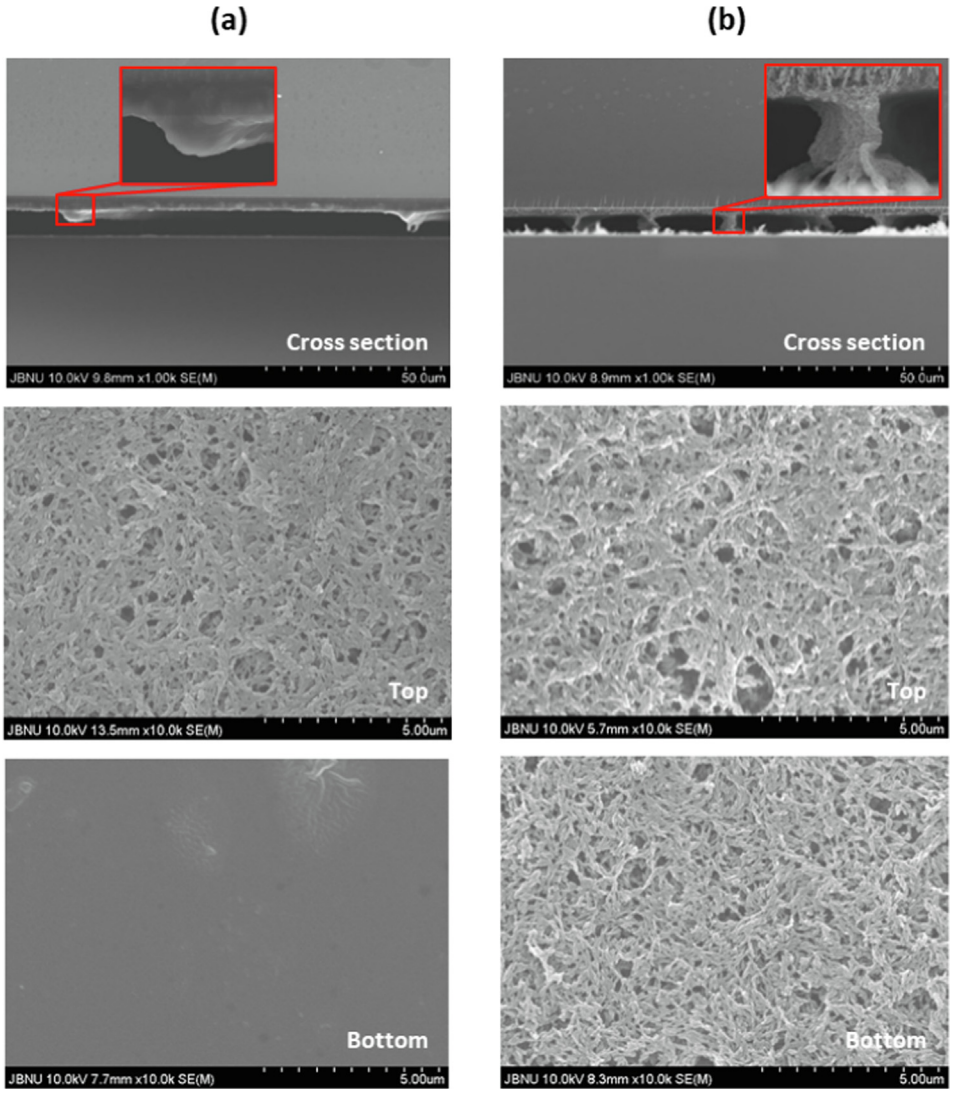

Fig. 7. FE-SEM images of polymer networks obtained by removing LCs from the cells. (a) Single-sided and (b) double-sided UV exposures at 50mW for 60 min. The red boxes are enlarged areas of polymer network observed in between glass substrates. (For interpretation of the references to colour in this figure legend, the reader is referred to the web version of this article.)

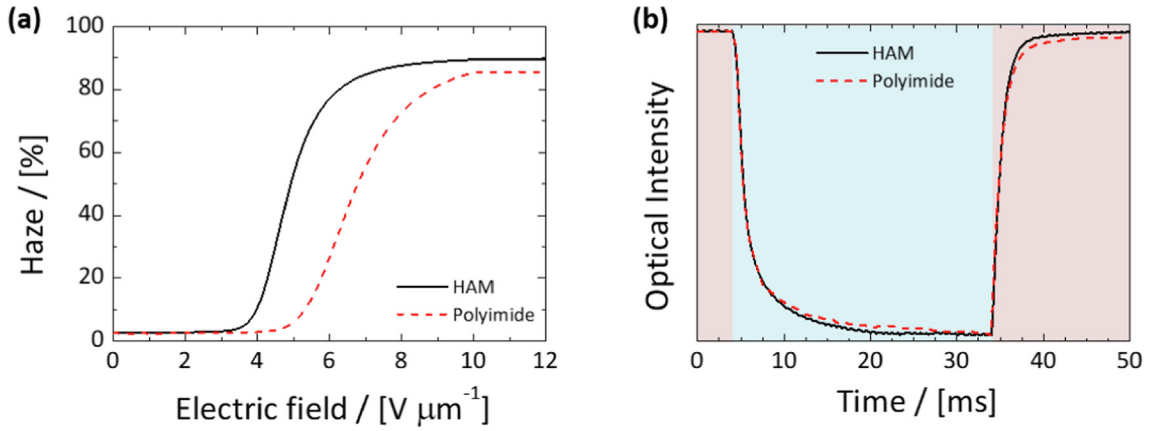

Fig. 8. (a) The electric field strength-dependent haze curves and (b) time-dependent transmittance curves in the demonstrated cells with HAM and polyimide.

solve one of the biggest challenges in application to energy-saving smart windows.

CRediT authorship contribution statement

Young Jin Lim: Methodology, Writing – original draft. **Minji Kang:** Investigation. **Hyun Soo Jeon:** Investigation. **MinSu Kim:** Methodology, Formal analysis, Writing – original draft, Writing – review & editing, Supervision, Funding acquisition. **Seung Hee Lee:** Conceptualization, Writing – review & editing, Supervision, Funding acquisition.

Data availability

Data will be made available on request.

Declaration of Competing Interest

The authors declare that they have no known competing financial interests or personal relationships that could have appeared to influence the work reported in this paper.

Acknowledgements

This research was supported by Basic Science Research Program through the National Research Foundation (NRF), Korea, funded by the Ministry of Education [2021R1I1A1A01049967] and [2021R1I1A1A01060001], and by ITECH R&D Program of MOTIE/KEIT (Ministry of Trade, Industry & Energy/Korea Evaluation Institute of Industrial Technology) [20012555] and [20016808].

References

[1] R.L. Sutherland, V.P. Tondiglia, L.V. Natarajan, T.J. Bunning, W.W. Adams, Electrically switchable volume gratings in polymer-dispersed liquid crystals, Appl. Phys. Lett. 64 (1998) 1074, https://doi.org/10.1063/1.110936.
[2] B. Wu, J.L. West, J.W. Doane, Angular discrimination of light transmission through polymer-dispersed liquid-crystal films, J. Appl. Phys. 62 (1998) 3925, https://doi.org/10.1063/1.339211.
[3] R. Ondris-Crawford, E.P. Boyko, B.G. Wagner, J.H. Erdmann, S. Žumer, J.W. Doane, Microscope textures of nematic droplets in polymer dispersed liquid crystals, J. Appl. Phys. 69 (1998) 6380, https://doi.org/10.1063/1.348840.
[4] M.J. Coles, C. Carboni, H.J. Coles, A highly bistable fast-shear aligned polymer dispersed ferroelectric liquid crystal device, Liq. Cryst. 26 (1999) 679–684, https://doi.org/10.1080/026782999204732.
[5] C.C. Bowley, G.P. Crawford, Diffusion kinetics of formation of holographic polymer-dispersed liquid crystal display materials, Appl. Phys. Lett. 76 (2000) 2235, https://doi.org/10.1063/1.126306.
[6] P. Drzaic, P.S. Drzaic, Putting liquid crystal droplets to work: a short history of polymer dispersed liquid crystals, Liq. Cryst. 33 (2011) 1281–1296, https://doi.org/10.1080/02678290601140563.
[7] J.-H. Lee, J.J. Lee, S.H. Lee, S.-W. Kang, S. Kundu, Y.J. Lim, Enhanced contrast ratio and viewing angle of polymer-stabilized liquid crystal via refractive index matching between liquid crystal and polymer network, Opt. Express. 21 (2013) 26914–26920, https://doi.org/10.1364/OE.21.026914.
[8] J. Heo, J.-W. Huh, T.-H. Yoon, Fast-switching initially-transparent liquid crystal light shutter with crossed patterned electrodes, AIP Adv. 5 (2015), https://doi.org/10.1063/1.4918277.
[9] J. Wang, C. Meng, Q. Gu, M.C. Tseng, S.T. Tang, H.S. Kwok, J. Cheng, Y. Zi, Normally transparent tribo-induced smart window, ACS Nano. 14 (2020) 3630–3639, https://doi.org/10.1021/ACSNANO.0C00107.
[10] M.S. Kim, F. Serra, Quasicrystalline arrays and moiré patterns in nematic liquid crystals for soft photonics, Adv. Opt. Mater. (2022) 2200916, https://doi.org/10.1002/ADOM.202200916.
[11] K.-H. Kim, B.W. Park, S.-W. Choi, J.-H. Lee, H. Kim, K.-C. Shin, H.S. Kim, T.-H. Yoon, Vertical alignment of liquid crystals without alignment layers, Liq. Cryst. 40 (2013) 391–395, https://doi.org/10.1080/02678292.2012.754961.
[12] S.-H. Lee, J.-H. Son, W.-C. Zin, S.H. Lee, J.-K. Song, Self-constructed stable liquid crystal alignment in a monomer-liquid crystal mixture system, Liq. Cryst. 39 (2012) 1049–1053, https://doi.org/10.1080/02678292.2012.693630.
[13] M.S. Kim, F. Serra, Tunable dynamic topological defect pattern formation in nematic liquid crystals, Adv. Opt. Mater. 8 (2020) 1900991, https://doi.org/10.1002/adom.201900991.
[14] S.-C. Jeng, C.-W. Kuo, H.-L. Wang, C.-C. Liao, Nanoparticles-induced vertical alignment in liquid crystal cell, Appl. Phys. Lett. 91 (2007), https://doi.org/10.1063/1.2768309.
[15] S.-J. Hwang, S.-C. Jeng, C.-Y. Yang, C.-W. Kuo, C.-C. Liao, Characteristics of nanoparticle-doped homeotropic liquid crystal devices, J. Phys. D. Appl. Phys. 42 (2008), https://doi.org/10.1088/0022-3727/42/2/025102.
[16] C.-W. Kuo, C.-C. Liao, S.-C. Jeng, W.-K. Chin, W.-Y. Teng, Y.-R. Lin, Nanoparticles-doped guest-host liquid crystal displays, Opt. Lett. 33 (2008) 1663–1665, https://doi.org/10.1364/OL.33.001663.
[17] H. Endo, Y. Katano, F. Kondo, K. Ogita, H. Tanaka, M. Yano, Development of self-alignment LC mixture for vertical alignment mode without polyimide alignment layer, in: Proc. Int. Disp. Work., International Display Workshops, 2017: pp. 175–177.
[18] Y.J. Lim, J.H. Lee, G.Y. Lee, M. Jo, E.J. Kim, T.H. Kim, M.S. Kim, M.-H. Lee, S.H. Lee, Polyimide-free vertical alignment in a binary mixture consisting of nematic liquid crystal and reactive mesogen: Pretilt modulation via two-step polymerization, J. Mol. Liq. 340 (2021), https://doi.org/10.1016/J.MOLLIQ.2021.117302.
[19] M.S. Kim, L.C. Chien, Topology-mediated electro-optical behaviour of a wide-temperature liquid crystalline amorphous blue phase, Soft Matter. 11 (2015) 8013–8018, https://doi.org/10.1039/c5sm01918d.
[20] R. Manda, S. Pagidi, M.S. Kim, C.H. Park, H.S. Yoo, K. Sandeep, Y.J. Lim, S.H. Lee, Effect of monomer concentration and functionality on electro-optical properties of polymer-stabilised optically isotropic liquid crystals, Liq. Cryst. 45 (2018) 736–745, https://doi.org/10.1080/02678292.2017.1380239.
[21] R. Manda, S. Pagidi, Y.J. Heo, Y.J. Lim, M.S. Kim, S.H. Lee, Polymer-stabilized monodomain blue phase diffraction grating, Adv. Mater. Interfaces 7 (2020) 1901923, https://doi.org/10.1002/ADMI.201901923.
[22] R. Manda, S. Pagidi, Y. Heo, Y.J. Lim, M.S. Kim, S.H. Lee, Electrically tunable photonic band gap structure in monodomain blue-phase liquid crystals, NPG Asia Mater. 12 (2020) 1–9, https://doi.org/10.1038/s41427-020-0225-8.
[23] N.H. Park, S.C. Noh, P. Nayek, M.H. Lee, M.S. Kim, L.C. Chien, J.H. Lee, B.K. Kim, S. H. Lee, Optically isotropic liquid crystal mixtures and their application to high-performance liquid crystal devices, doi: 10.1080/02678292.2015.1006698.
[24] S. Pagidi, R. Manda, H.S. Shin, J. Lee, Y.J. Lim, M.S. Kim, S.H. Lee, Enhanced electro-optic characteristics of polymer-dispersed nano-sized liquid crystal droplets utilizing PEDOT:PSS polymer composite, J. Mol. Liq. 322 (2021), https://doi.org/10.1016/J.MOLLIQ.2020.114959.
[25] M.S. Kim, R. Manda, D.Y. Lee, J.W. Lee, A. Nauman, H.R. Kim, S.H. Lee, Field-induced structural transitions in liquid crystal microemulsions, Adv. Opt. Mater. 10 (2022) 2200563, https://doi.org/10.1002/ADOM.202200563.
[26] S.L. Lee, M.S. Kim, D.Y. Lee, Y.H. Lin, S.H. Lee, Optically isotropic nano-size encapsulation of nematic liquid crystals with a high-filling factor, J. Mol. Liq. 359 (2022), https://doi.org/10.1016/J.MOLLIQ.2022.119254.
[27] D.B. Chung, H. Tsuda, H. Chida, A. Mochizuki, Effects and structural model of surfactants on the hysteresis behavior of polymer dispersed liquid crystals, Mol. Cryst. Liq. Cryst. Sci. Technol. Sect. A. Mol. Cryst. Liq. Cryst. 304 (1997) 81–87, https://doi.org/10.1080/10587259708046946.
[28] Y. Li, Z. Yang, R. Chen, L. Mo, J. Li, M. Hu, S.-T. Wu, Submillisecond-response polymer network liquid crystal phase modulators, Polym. 12 (2020) 2862, doi: 10.3390/POLYM12122862.